UCRL-JC-133133
PREPRINT

Nitrogen Implantation Effects on the Chemical Bonding and Hardness of Boron and Boron Nitride Coatings

Alan Jankowski
Thomas Felter
Robert Patterson
Jeffrey Hayes
Simone Anders
Thomas Stamler
David Poker

This paper was prepared for submittal to the
Materials Research Society
Boston, MA
November 30 - December 2, 1998

February 8, 1999

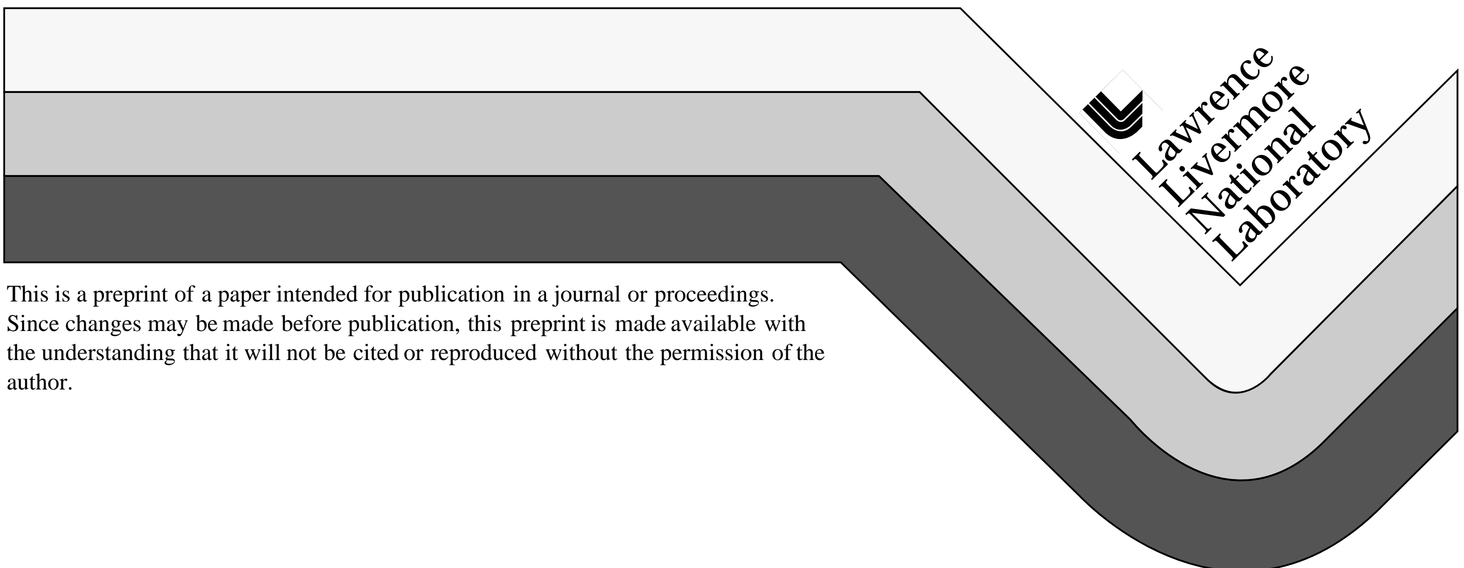

This is a preprint of a paper intended for publication in a journal or proceedings. Since changes may be made before publication, this preprint is made available with the understanding that it will not be cited or reproduced without the permission of the author.

DISCLAIMER

This document was prepared as an account of work sponsored by an agency of the United States Government. Neither the United States Government nor the University of California nor any of their employees, makes any warranty, express or implied, or assumes any legal liability or responsibility for the accuracy, completeness, or usefulness of any information, apparatus, product, or process disclosed, or represents that its use would not infringe privately owned rights. Reference herein to any specific commercial product, process, or service by trade name, trademark, manufacturer, or otherwise, does not necessarily constitute or imply its endorsement, recommendation, or favoring by the United States Government or the University of California. The views and opinions of authors expressed herein do not necessarily state or reflect those of the United States Government or the University of California, and shall not be used for advertising or product endorsement purposes.

NITROGEN IMPLANTATION EFFECTS ON THE CHEMICAL BONDING AND HARDNESS OF BORON AND BORON NITRIDE COATINGS

Alan Jankowski*, Thomas Felter*, Robert Patterson*, Jeffrey Hayes*, Simone Anders**, Thomas Stamler**, and David Poker***
*Lawrence Livermore National Laboratory, 7000 East Avenue, Livermore, CA 94550
**Lawrence Berkeley National Laboratory, 1 Cyclotron Road, Berkeley, CA 94720
***Oak Ridge National Laboratory, 1 Bethel Valley Road , Oak Ridge, TN 37831

ABSTRACT

Boron nitride (BN) coatings are deposited by the reactive sputtering of fully dense, boron (B) targets utilizing an argon-nitrogen (Ar-N_2) reactive gas mixture. Near-edge x-ray absorption fine structure analysis reveals features of chemical bonding in the B 1*s* photoabsorption spectrum. Hardness is measured at the film surface using nanoindentation. The BN coatings prepared at low, sputter gas pressure with substrate heating are found to have bonding characteristic of a defected hexagonal phase. The coatings are subjected to post-deposition nitrogen (N^+ and N_2^+) implantation at different energies and current densities. The changes in film hardness attributed to the implantation can be correlated to changes observed in the B 1*s* NEXAFS spectra.

INTRODUCTION

Boron nitride (BN) is of interest for use in wear resistant coatings and hard surfaces. The hardness of crystalline films is directly related to the microstructure and chemical bonding within the material. Near-edge x-ray absorption fine structure (NEXAFS) spectroscopy can be used to identify the nature of chemical bonding in a material. For boron and its nitride phases, chemical bonding features are shown to correlate with the hardness of crystalline and nanocrystalline BN as well as amorphous B films.[1-4] Curve fitting the NEXAFS spectra beyond the σ^*-edge can be used to determine the relative sp^2 and sp^3 intensities that in turn provides a quantification of the BN phase content.[1,4] An increase in hardness is found to be proportional with the increase in the cubic boron-nitride (cBN) phase content for sputter deposited BN films.[4]

The variation of deposition conditions (i.e. sputter gas pressure, flow and composition along with substrate temperature and applied bias) affect the formation of crystalline phases in BN films deposited by rf sputtering pure boron targets using unbalanced planar magnetrons.[1,2] Hardness can be influenced by post-deposition treatments as well. A post deposition implantation of boron and boron nitride can reveal the nature of formation and stabilization of the cubic boron nitride (cBN) phase. Ion implantation of hexagonal boron nitride (hBN) with N_2^+ was shown with NEXAFS to induce a significant proportion of sp^3 bonding characteristic of cBN.[3] A 100-fold variation in hardness appears for BN films that can be characterized by sp^2 bonding features alone.[2] The presence of defects in the chemical bonding of hBN appear as resonances found beyond the π^*-edge.[3-4] The present objective is to further evaluate the effects of implantation energy and current density on boron and its nitride phases. In particular, to use post deposition implantation to harden B and hBN coatings.

EXPERIMENTALS

The BN (no. 417a, 417b and 814) and B (no. 819) samples are prepared using physical vapor deposition. The 0.4-0.8μm thick coatings are deposited by sputtering pure boron using planar magnetrons operated at 200W power in the rf mode.[1-2,5] The boron targets are unique in that full (>99%) density is achieved with elemental purity (>0.998). Synthesis of the boron sputter targets is described in detail elsewhere.[6] The deposition chamber is cryogenically pumped to a 5×10^{-6} Pa base pressure. The B coatings are deposited using Ar as the working gas whereas the BN coatings are deposited using a Ar-25%N_2 reactive gas mixture.[5] A 10-20nm thick Cr layer is initially deposited to enhance coating adherence to the 1.2x1.2cm silicon substrates. The

substrates are positioned laterally from the center of the 6.3cm diameter target. A substrate temperature of 300˚C is achieved using a Boralectric™ heater. A 0.23Pa sputter gas pressure is maintained using a 28 cm^3 min^{-1} total flow rate. Deposition rates of 0.019 nm s^{-1} and 0.025 nm s^{-1} are produced using the Ar and Ar-25%N_2 sputter gases, respectively. The as-deposited coating thickness (t_o) is measured using a Dektak II contact profilometer.

The as-deposited samples are modified by nitrogen implantation. A tantalum shadow mask exposes the center of each coated wafer to the implanted species. Two sets of implants are performed that accentuate the effects of the per nitrogen implant energy and current density. The nitrogen implantations are achieved with a cryogenically pumped Varian 3000 system using a Freeman source. In the first set, the variable is implant energy. A two-pocket shadow mask is used for samples no. 417a and 417b. The terminal potential is set at 90 or 180 keV. A selection at the analyzer magnet of 14 atomic mass units (amu) is used for N^+ ions. These conditions yield 90 or 180 keV per incident nitrogen atom. A 24μA focused beam is rastered across a surface area in excess of 100 cm^2 that covers the hard-masked substrates. This exposure condition produces a 5.0×10^{14} cm^{-2} s^{-1} flux of nitrogen atoms, i.e. an equivalent "nitrogen atom" beam current density (ρ_N) of 81 μA cm^{-2}. The total dose of nitrogen atoms at either 90 or 180 keV is 1×10^{17} cm^{-2}. In the second implantation set, the variable is current density with respect to the first implant set. For this implant, a four-pocket shadow mask is used for samples no. 814 and 819. The terminal potential is set at 200 keV. A selection at the analyzer magnet of 28 amu is used for N_2^+ ions. These conditions yield 100 keV per incident nitrogen atom. A 15μA defocused beam is rastered across a surface area in excess of 100 cm^2 that covers the hard-masked substrates. This exposure condition produces a 1.9×10^{14} cm^{-2} s^{-1} flux of nitrogen atoms, i.e. an equivalent ρ_N of 31 μA cm^{-2}. The total dose of nitrogen atoms at 100 keV is 2×10^{17} cm^{-2}. Note that before this implant, the samples received a small 1.4×10^{16} cm^{-2} dose of 200 keV (N^+) nitrogen atoms as 14 amu was inadvertantly selected for the implant condition. The change in thickness (Δt) found in the implanted region is measured using a Dektak II contact profilometer. A summary of the implant conditions is listed in Table 1 for each sample wherein a suffix is added to each sample no. indicating the implantation energy per nitrogen atom. For example, the 90 keV implanted BN sample no. 417a is designated as 417-90.

Near-edge x-ray absorption fine structure (NEXAFS) spectroscopy provides information about the elemental composition and bonding character of the B and BN samples.[7] NEXAFS spectroscopy is based on the availability of x-ray radiation of tunable wavelength that is produced by a synchrotron. Measurements are taken on beamline 8.0 at the Advanced Light Source (ALS) in Berkeley. This undulator beamline is equipped with a spherical grating monochromator that delivers x-ray radiation in the range of 200-1500 eV with a resolving power of $E/\Delta E = 10^4$. NEXAFS spectroscopy is very sensitive to variations in the local bonding structure of boron nitride, and therefore is a suitable method to study the various phases of boron nitride.[4] Unique spectral features in the boron and nitrogen 1*s* photoabsorption cross sections correspond with resonances that are specific to discrete BN phases.[8] The photon energy of monochromatic synchrotron radiation is scanned through the core-level edge while monitoring the electron yield to measure the B 1*s* core-level photoabsorption cross-section. The low-energy, long mean-free-path electron emission dominates the signal. The transition of 1*s* initial states into p-like empty final states is associated with sp^2 hybridized, planar bonding that is characteristic of hBN and appears as the narrow, intense transition at 192 eV. This π^* resonance is absent in sp^3 tetrahedrally bonded materials such as cBN which uniquely evidence an absorption maximum step into σ^* continuum states above 194 eV. The resonance peak at 192 eV indicates B-(N_3) bonding in hBN. The presence of N-void defects in the hBN structure are representative of B-(BN_2) and B-(B_2N) corresponding to the successive satellite peaks above 192 eV.[3] The diffuse *peak* for elemental boron at 194 eV can be correlated with some degree of planarization of sp^3 tetrahedral bonding, similar in signature to the sub-surface boron layer that forms in silicon.[9-10] Local NEXAFS spectra of the implanted and unimplanted region are acquired by averaging over a 50 μm diameter region from each sample.

The mechanical properties of the B and BN samples are characterized using nanoindentation. Hardness measurements are performed on a Nano Instruments IIs nanoindenter. A Berkovitz diamond tip that has three-sides, each at 65.3˚ to the base, is used to indent the coatings. Force

measurements at various depths up to 1 micron are repeated between 10 to 15 times, then

Table I. Samples, Implant Conditions and Properties of B and BN Samples

Sample No.	Deposit	t_o (μm)	Ion	Energy (keVatom^{-1})	ρ_N (μAcm^{-2})	Δt (nm)	I_1 (B-N_3)	I_2 (B-BN_2)	I_3 (B-B_2N)	I_4 (B)	H (GPa)
417a-0	BN	0.42	-	0	0	0	0.81	0.13	0.05	0.01	0.9
417a-90	BN	0.42	N^+	90	81	-270	0.43	0.28	0.18	0.11	3.4
417b-0	BN	0.42	-	0	0	0	0.81	0.13	0.05	0.01	0.9
417b-180	BN	0.42	N^+	180	81	-140	0.92	0.06	0.02	0.00	0.2
814-100	BN	0.80	N_2^+	100	31	+33	-	-	-	-	0.7-4.0
ref.[2,10]	B	0.14	-	0	0	0	0.00	0.01	0.03	0.96	26.4
ref.[5]	B	6.0	-	0	0	0	-	-	-	-	28.3
819-100	B	0.48	N_2^+	100	31	+33	-	-	-	-	40.1

averaged, and the standard deviations are used to derive the probable errors. Hardness is defined as the average pressure under the indenter tip. Hardness can be calculated from the load divided by the projected area of contact between the tip and the sample. The projected area is determined from the depth of penetration using the known profile of the tip. Since indentation depth is a combination of elastic and inelastic components, a proper derivation of hardness requires the removal of the elastic portion. The detailed computation of hardness from load-displacement curves developed for bulk homogeneous materials has continued to evolve to better define parameters such as true contact area that are useful for analyzing stiff materials as well as inhomogeneous systems.[11-12] Although there are limitations imposed by analyzing inhomogeneous and hard materials, hardness is computed using the standard procedure developed from Doerner and Nix.[13-15] The elastic modulus is calculated from the initial linear portion of the unloading curve and extrapolates to zero load.

RESULTS

The NEXAFS spectra for samples no. 417a-0 (Fig. 1) and 417b-0 compared with reference data from Jiménez, et al.[4,10] show that the unimplanted area exhibits bonding typical of the hexagonal structure with the boron π* resonance at 192 eV (peak 1). The spectrum is very similar to published spectra of BN films grown by either pulsed-laser or rf-sputter deposition.[4] The small additional features (peaks 2-4) just above the boron π* resonance are correlated with N-void defects in the hexagonal bonding, i.e. with the fact that boron atoms can be bound to three (peak 1), two (peak 2), one (peak 3), or no (peak 4) nitrogen atoms leading to four different peaks at the π* resonance. The spectra for a B film is shown for reference.[10] Whereas the spectrum for the 180 keV implant region (sample no. 417b-180 not shown) evidences a very small decrease in the N-void defect peak intensities relative to the unimplanted condition, the spectrum for the 90 keV implant region (sample no. 417a-90) exhibits stronger defect features. No clear formation of the cubic phase is found in the sample no. 417 set of films as is observed when films are deposited by ion-assisted laser deposition at lower (10-70 μA cm^{-2}) current densities of nitrogen.[1,4] The peak intensities (**I**) of the B 1s spectra are quantified for each BN bonding variant, i.e. peaks 1-4. A fitting procedure is applied to deconvolute the π* resonance peaks into a superposition of four Gaussian curves.[2-3] The results using this fitting procedure are listed in Table 1 for each sample. NEXAFS spectra await for samples 814 and 819.

The hardness measured for each sample (Fig. 2) increases with the indenter depth. The hardness values converge to the 9-10 GPa value of the Si substrate beyond an indenter depth equal to the film thickness. To measure the film requires attention to the shallow (about 10% t_o) indentation depths.[16] The average hardness (**H**) values measured for all B and BN samples are listed in Table 1. The hardest as-deposited sample is the thin B coating.[2] Similar 28±1 GPa hardness values are measured for 6μm thick B films using a Vickers micro-indenter.[5] The

softest sample is implanted BN no. 417b-180. The hardness of an *unimplanted* region of BN samples no. 417a-90 and 417b-180 are equal to the as-deposited value of 0.9 GPa for samples

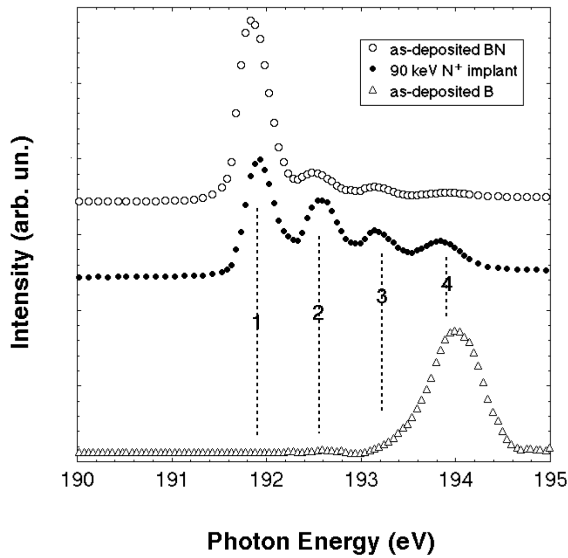

Fig. 1. Electron yield intensity varies with photon energy (eV) in these NEXAFS B 1*s* spectra for B (ref.)[10], as-deposited BN (417a-0) and 90keV N^+ implanted BN (417a-90).

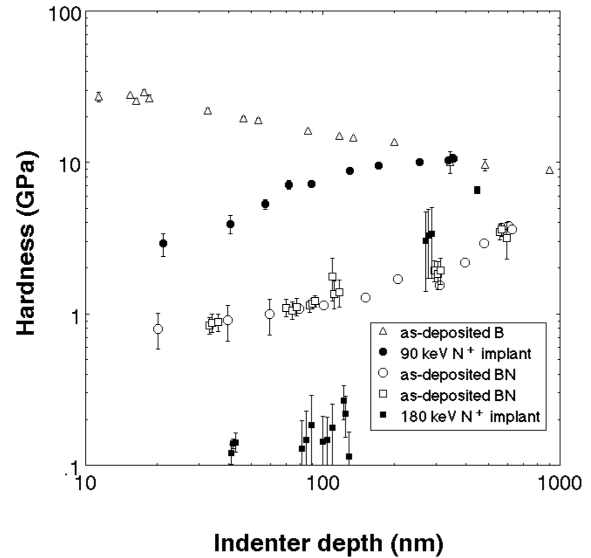

Fig. 2. Hardness (GPa) varies with indenter depth (nm) for B (ref.)[2], as-deposited BN (417a-0 and 417b-0), and N^+ implanted BN at 90 keV (417a-90) and 180 keV (417b-180).

no. 417a-0 and 417b-0 as expected. The 90 keV N^+ implant hardens the BN coating surface whereas the 180 keV N^+ implant softens the BN coating surface.

The 200 keV N_2^+ implant shows some unusual results for samples no. 814 and 819. Most interesting is the 12 GPa increase in hardness measured for B sample no. 819-100. The hardness values do not appear to signifcantly differ between the implanted and unimplanted regions of sample no. 819-100. Since the hardness of B is well-established[2,5] this raises concern to the certainty of the as-deposited region associated with the sample no. 819 hardness measurement. Also, a similar irregularity is found for the hardness measured in the unimplanted region of sample no. 814. A 0.7 to 4 GPa range in hardness is measured for sample no. 814-100. This broad range draws attention to the relative etching and spallation that occurs during implantation. If the soft BN surfaces are hardened by the implant at a low current density, then there will be little etching but perhaps some spallation of the hard surface off the softer base material. Thus, some areas of the implant region (i.e. sample no. 814-100) may appear hard and others soft as the as-deposited BN. If the nitrogen current density is high, thereby annealing the implanted surface, then a significant etching rate may result (as for sample no. 417a-90). Thus, it can be postulated that a 0.7 GPa hardness is likely for sample no. 814-0 as is consistent with all prior measurements for as-deposited BN. The hardness of sample no. 814-100 is likely ≤4.0 GPa, showing a several-fold increase from the as-deposited condition as is similarly found for the implanted sample no. 417a-90. Cubic BN does not form for any of the implanted BN samples. However, the 200 keV N_2^+ implant of B sample no. 819 may result in some sp^3 bonding in the BN surface.

DISCUSSION

The comparative hardness of BN samples no. 417a and 417b correspond with the relative peak intensities of the π* resonances. The hardest films have a strong B peak intensity whereas the softest films have strong B-(N_3) bonding. An empirical model is recently developed to directly relate the relative peak intensities to the film hardness.[17] Stabilization of the cBN phase in thin films can be achieved through the use of ion-assisted deposition techniques, e.g.

high voltage, bias sputtering or ion beam bombardment at the substrate.[18-21] Mechanisms proposed for cBN stabilization in BN films include both preferential sputtering effects[22], the presence of large stresses[23-24] and subplantation[25-26] wherein low energy ions are implanted below the surface to increase local density. Post deposition treatments of hBN are also revealing, as 180 keV N_2^+ ion implantation at a 10 μA cm^{-2} current density induced a significant proportion of sp^3 bonding characteristic of cBN.[3] Whereas N-void defect introduction to the BN film is evident in the π*-resonances, there are no noticeable changes in the B 1*s* spectra beyond the σ*-edge indicative of sp^3 bonding at the higher (31 or 81 μA cm^{-2}) current densities used in this study. However, the 31μA cm^{-2} beam condition may harden the as-deposited BN film more than the 81μA cm^{-2} beam condition. The effect of current density is also seen in preferential etching, perhaps similar to plasma-assisted chemical vapor deposition processes wherein the growth of the cBN phase can occur competitively with the selective etching of the sp^2 (hBN) phase during film growth.[27] Thus it appears an ion current threshold exists for cBN formation. A higher energy (180 keV N^+) ion implant at the greater current density can effectively anneal out the N-void defect structure hence decrease the film hardness. Thus, examination with core level photoabsorption to study BN defects and metastable bonding configurations confirms that the presence of point defects support mechanisms involving defect creation in cBN formation.[3-4] Recently, similar findings requiring defect generation are found in the mass and energy measurement of species responsible for cBN growth in rf bias sputter conditions.[28-29]

SUMMARY

B and BN coatings sputter deposited from pure B targets at low gas pressure and temperature are N ion implanted. The coatings are characterized with NEXAFS and nanoindentation to reveal chemical bonding and surface hardness, respectively. The as-deposited BN coatings have defected hBN bonding and a 0.7-0.9 GPa surface hardness. A high energy, high current density, N implant etches and softens the BN coatings to a relaxed state of hBN bonding with a 0.2 GPa hardness. A low energy implant hardens the BN coatings with an increase in (N-void) defect structure and an increase in hardness to 3.4-4.0 GPa (where a lower current density enhances the effect). The as-deposited B coating is amorphous[5,10] and has a 26-28 GPa surface hardness. The low energy, low current density, N implant hardens the B coating to 40 GPa. Future NEXAFS analysis will probe for the presence of sp^3 bonding in this N implanted B coating. The post deposition, N implantation yields results similar to ion-beam assisted deposition and ion implantation studies in which stabilization of cBN occurs during growth.[3-4,25-26]

ACKNOWLEDGMENTS

This work was performed under the auspices of the United States Department of Energy by Lawrence Livermore National Laboratory under contract No. W-7405-Eng-48. This work was supported by the U.S. Department of Energy, Office of Basic Energy Sciences under contract No. DE-AC03-765F00098 and by the Synthesis and Processing Center for Surface Hardness.

REFERENCES

1. A. Jankowski, J. Hayes, M. McKernan and D. Makowiecki, Thin Solid Films **308-309**, p. 94 (1997).

2. A. Jankowski and J.P. Hayes, Diamond Relat. Mater. **7**, p. 380 (1997).

3. I. Jiménez, A. Jankowski, L. Terminello, J. Carlisle, D. Sutherland, G. Doll, J. Mantese, W. Tong, D. Shuh and F. Himpsel, Appl. Phys. Lett. **68**, p. 2,816 (1996).

4. I. Jiménez, A. Jankowski, L. Terminello, D. Sutherland, J. Carlisle, G. Doll, W. Tong, D. Shuh, and F. Himpsel, Phys. Rev. B **55**, p. 12,025 (1997).

5. M. McKernan, D. Makowiecki, P. Ramsey and A. Jankowski, Surf. Coatings Technol. **49**, p. 411 (1991).

6. D. Makowiecki and M. McKernan, *Fabrication of Boron Sputter Targets*, U.S. Patent No. 5,392,981 (February 28, 1995).

7. J. Stöhr, *NEXAFS Spectroscopy*, Springer, New York, NY (1992).

8. L. Terminello, A. Chaiken, D. Lapiano-Smith, G. Doll and T. Sato, J. Vac. Sci. Technol. A **12**, p. 2,462 (1994).

9. A. McLean, L. Terminello and F. Himpsel, Phys. Rev. B **41**, p. 7,694 (1990).

10. A. Jankowski, I. Jiménez, J. Hayes, D. Shuh, D. Sutherland, J. Carlisle, L. Terminello and F. Himpsel, in *Applications of Synchrotron Radiation to Materials Science III*, edited by L. Terminello, S. Mini, D. Perry and H. Ade (Mater. Res. Soc. Proc. **437**, Pittsburgh, PA, 1996), p. 207-210.

11. J. Loubet, J. Georges and J. Meille, in *Microindentation Techniques in Materials Science and Engineering*, edited by P. Blau and B. Lawn (American Society for Testing and Materials, Philadelphia, PA, 1986), p. 72-89.

12. S. Hainsworth, H. Chandler and T. Page, J. Mater. Res. **11**, p. 1,987 (1996).

13. M. Doerner and W. Nix, J. Mater. Res. **1**, p. 601 (1986).

14. G. Pharr, W. Oliver and F. Brotzen, J. Mater. Res. **7**, p. 613 (1992).

15. W. Oliver and G. Pharr, J. Mater. Res. **7**, p. 1,564 (1992).

16. ASTM Standard E 92, in *Annual Book of Standards 3.01*, American Society for Testing and Materials, Philadelphia, PA, p. 264 (1987).

17. A. Jankowski, Thin Solid Films, in press (1998).

18. D. Kester, K. Alley, D. Lichtenwainer and R. Davis, J. Vac.Sci.Technol. A**12**, p.3074 (1994).

19. T. Friedmann, P. Mirkarimi, D. Medlin, K. McCarty, E. Klaus, D. Boehme, H. Johnsen, M. Mills, D. Ottesen and J. Barbour, J. Appl. Phys. **76**, p. 3,088 (1994).

20. T. Wada and N. Yamashita, J. Vac. Sci. Technol. A **10**, p. 515 (1992).

21. N. Tanabe, T. Hayashi and M. Iwaki, Diamond Relat. Mater. **1**, p. 883 (1992).

22. S. Reinke, M. Kuhr and W. Kulisch, Diamond Relat. Mater. **3**, p. 341 (1994).

23. D. McKenzie, W. McFall, W. Sainty, C. Davis and R. Collins, Diamond Relat. Mater. **2**, p. 970 (1993).

24. D. Medlin, T. Friedmann, P. Mirkarimi, P. Rez, M. Mills and K. McCarty, J. Appl. Phys. **76**, p. 295 (1994).

25. J. Robertson, Diamond Relat. Mater. **5**, p. 519 (1996).

26. S. Ulrich, J. Schwan, W. Donner and H. Ehrhardt, Diamond Relat. Mater. **5**, p. 548 (1996).

27. I. Konyashin, J. Loeffler, J. Bill and F. Aldinger, Thin Solid Films **308-309**, p. 101 (1997).

28. Y. Yamada, Y. Tatebayashi, O. Tsuda and T. Yoshida, Thin Solid Films **295**, p. 137 (1997).

29. O. Tsuda, Y. Tatebayashi, Y.Yamada-Takamura and T. Yoshida, J. Vac. Sci. Tecnol. A **15**, p. 2,859 (1997).